Lipidomic analysis of epithelial corneal cells following hyperosmolarity and benzalkonium chloride exposure: New insights in dry eye disease

Romain Magny, Karima Kessal, Anne Regazzetti, Asma Ben Yedder, Christophe Baudouin, Stéphane Mélik Parsadaniantz, Françoise Brignole-Baudouin, Olivier Laprévote, Nicolas Auzeil

Lipidomic analysis of epithelial corneal cells following hyperosmolarity and benzalkonium chloride exposure: new insights in dry eye disease

Romain Magny[1,2], Karima Kessal[1,3], Anne Regazzetti[2], Asma Ben Yedder[1], Christophe Baudouin[1,3,4], Stéphane Mélik Parsadaniantz[1], Françoise Brignole-Baudouin[1,2,3] Olivier Laprévote[2,5] and Nicolas Auzeil[2]

[1]Sorbonne Université UM80, INSERM UMR 968, CNRS UMR 7210, Institut de la Vision, IHU Foresight, Paris, France.

[2]Chimie Toxicologie Analytique et Cellulaire CNRS UMR 8038, Université Paris Descartes, Faculté de Pharmacie, Sorbonne Paris Cité, Paris, France.

[3]Centre Hospitalier National d'Ophtalmologie des Quinze-Vingts, Paris, France.

[4]Hôpital Ambroise Paré, APHP, Université Versailles Saint-Quentin-en-Yvelines, Boulogne-Billancourt, France.

[5]Hôpital Européen Georges Pompidou, AP-HP, Service de Biochimie, Paris, France.

Corresponding authors: nicolas.auzeil@parisdescartes.fr

Abstract

Dry eye disease (DED) is a multifactorial chronic inflammatory disease of the ocular surface characterized by tear film instability, hyperosmolarity, cell damage and inflammation. Hyperosmolarity is strongly established as the core mechanism of the DED. Benzalkonium chloride (BAK) - a quaternary ammonium salt commonly used in eye drops for its microbicidal properties - is well known to favor the onset of DED. Currently, little data are available regarding lipid metabolism alteration in ocular surface epithelial cells in the course of DED. Our aim was to explore the effects of benzalkonium chloride or hyperosmolarity exposure on the human corneal epithelial (HCE) cell lipidome, two different conditions used as *in vitro* models of DED. For this purpose, we performed a lipidomic analysis using UPLC-HRMS-ESI+/-. Our results demonstrated that BAK or hyperosmolarity induced important modifications in HCE lipidome including major changes in sphingolipids, glycerolipids and glycerophospholipids. For both exposures, an increase in ceramide was especially exhibited. Hyperosmolarity specifically induced triglyceride accumulation resulting in lipid droplet formation. Conversely, BAK induced an increase in lysophospholipids and a decrease in phospholipids. This lipidomic study highlights the lipid changes involved in inflammatory responses following BAK or hyperosmolarity exposures. Thereby, lipid research appears of great interest, as it could lead to the discovery of new biomarkers and therapeutic targets for the diagnosis and treatment of dry eye disease.

Key words: Dry eye, lipidomic analysis, benzalkonium chloride, hyperosmolarity stress, UPLC-HRMS

Highlights

- BAK and HO profoundly affect the lipidome of epithelial corneal cells
- Cell levels of bioactive lipids involved in inflammatory pathways are modified
- Both BAK and HO increase levels of ceramide species
- HO induces lipid droplets and increases phospholipid biosynthesis
- BAK decreases cell phospholipid levels in favor of their lysophosphatidic forms

1. Introduction

Dry eye disease (DED) is a multifactorial chronic inflammatory disease of the ocular surface, affecting 20% of the population [1]. Its incidence is in constant growth, affecting millions of people worldwide. DED results in visual disorders and neurosensory abnormalities - discomfort sensations, burning, itching and pain - and alters occupational performances and quality of life. DED has been defined as "*a multifactorial disease of the ocular surface characterized by a loss of homeostasis of the tear film, and accompanied by ocular symptoms, in which tear film instability and hyperosmolarity, ocular surface inflammation and damage, and neurosensory abnormalities play etiological roles*" [2]. DED is furthermore self-maintained by a vicious circle, enclosing alteration of tear film, hyperosmolarity, inflammation of the ocular surface leading to release of pro-inflammatory cytokines such as IFNγ, TNFα, IL-1β or IL-6 [3–7].

Hyperosmolarity (HO), known to be the core mechanism of DED, contributes to promoting and/or nurturing the pathology [2,5]. DED etiology includes autoimmune origin such as in Sjögren syndrome and also exogenous causes such as exposure to environmental toxics or iatrogenic agents [8]. DED onset may also be related to the toxic effect of preservatives required by the pharmacopeia guidelines as excipients in multidose eyedrops, the most common of them being benzalkonium chloride (BAK) [8,9]. BAK is a quaternary ammonium salt with detergent and microbicidal properties and quaternary ammonium compounds are widely found in disinfecting sprays both at home and at work [10]. Initially described in glaucomatous patients who are constrained to a chronic eyedrop administration [9,11], BAK toxicity impacts the different structures of the ocular surface, the conjunctiva, the cornea but also deeper structures such as the trabecular meshwork, the lens or even the retina [12,13]. In addition, because of its pro-inflammatory, pro-apoptotic and pro-oxidative effects, BAK may be responsible for DED or worsen it [14–16].

The ocular surface epithelial cells represent a physiological barrier playing a key role in the protection of the eye. Indeed, corneal and conjunctival cells are the first impacted during the alteration of the tear film contributing to the pathophysiology of DED. Many molecular mediators involved in

DED pathophysiology have been widely described in *in vitro* models [2,6,17]. Indeed, corneal and conjunctival cells exposed to BAK or HO undergo deleterious effects, especially apoptosis and oxidative stress [18–22]. In addition, an increase in cytokines such as IL-1β, TNFα, IL-6, chemokines such as CCL2 or matrix metalloproteases (MMP) such as MMP9, which are all pro-inflammatory molecular features of the DED pathology, was reported in these models [21,23,24].

Both inflammatory processes and cell death phenomena may involve second messengers derived from lipids. Indeed, lipids are not only the key components of biological cell membranes as well as sources of energy, they are also key mediators of intercellular and intracellular processes [25–27]. During the last two decades, some of them have been described as "bioactive lipids" tightly associated with several chronic diseases including diabetes, inflammatory bowel disease, multiple sclerosis, atherosclerosis [28,29]. Several studies have been dedicated to the role of lipids in ocular pathologies. An increase in sphingolipid abundance was thus reported in the cornea of diabetic patients [30]. In addition, Robciuc *et al.* reported the role of lipids in ocular pathologies highlighting the importance of sphingolipid homeostasis [31]. During DED, lipid composition of the tear film, which is under control of the meibomius gland secretion, is altered as it was previously shown by several studies focusing on its lipid characterization [32–35]. In contrast, to our knowledge, no study aimed at describing the modulation of epithelial cell lipids, involved in cell death process and promoting inflammatory cell recruitment, and its pathophysiological consequences in DED.

The purpose of this study was to characterize the changes of the lipid composition in a human epithelial corneal cell line following BAK or HO exposure, two well-known distinct stressors acting on cell membranes [36,37]. The aim was also to understand their differential effects on cell-membrane lipids and *in fine*, to identify lipid species as possible key markers of DED. Based on cytotoxicity assay and on gene expression of proinflammatory cytokines, we first determined the osmolarity levels and BAK concentrations to be used for cell exposures. We then performed a comprehensive lipidomic analysis to characterize qualitatively and quantitatively the changes occurring in the cellular lipid

93 profile resulting either from HO or BAK exposures. Finally, to support lipidomic analysis results, we
94 assessed the gene expression of enzymes involved in the modulated lipid biosynthesis.

2. Material and Methods

2.1. Cell line and culture conditions

Human corneal epithelial cell line (HCE) was obtained from the RIKEN biobank (Tsukuba, Japan) [38]. HCE cells were grown in culture flasks using DMEM/F12 (1/1), 10% fetal bovine serum (FBS), 2 mM glutamine, 100 U/mL penicillin and 100 µg/mL streptomycin all from Gibco (Paisley, UK). At confluence, every 3 days, cells were harvested with trypsin-EDTA 0.05% in dubelco phosphate-buffered saline (DPBS). Cells were used in this study from passages 3 to 12.

2.2. Exposure solutions

A stock solution of 0.1% (w/v) BAK (Sigma, Saint Quentin Fallavier, France) corresponding to 2.65 mM was used to prepare the 10^{-4}% BAK exposure solution, one hundred times lesser than the average concentration used in standard eye drop formulations. The 500 mOsM solutions were obtained after dilution of a 1000 mOsM stock solution prepared by overloading the culture medium with sodium chloride (Sigma-Aldrich, Saint Quentin Fallavier, France). Medium osmolarity was controlled using an osmometer Roebling 13DR (Roebling, Berlin, Germany).

2.3. Cell viability assay

Neutral Red (NR) uptake assay is based on the lysosome staining of viable cells after uptake of the dye through an active transport. To assess viability of HCE cells after exposure to HO or BAK, a solution of NR at 50 µg/mL was added to the cells grown at subconfluence in a 96-wells plate (20.000 cells/well), we performed NR assay, in accordance with previously published data [39]. The solution of NR was left to incubate for 3h at 37°C. Cells were washed with DPBS, then lysed using a mixture containing water, ethanol, acetic acid (49.5/49.5/1, v/v/v) and finally homogenized at room temperature for 15 minutes on a stirring plate. Fluorescence intensity was measured using a spectrofluorometer Infinite® 1000 (TECAN, Neuville-Sur-Oise, France) at 540 nm excitation and 600 nm emission wavelengths.

2.4. Reactive oxygen species production

ROS production was determined using 2',7'-Dichlorohydrofluorescein diacetate (H_2DCFDA) assay. The H_2DCFDA 0.1 M stock solution in DMSO (Thermo Fisher Scientific, Saint-Quentin-Fallavier, France) was used to prepare a 20 µM solution in DPBS. Cells were incubated for 24 hours with BAK or under HO condition on a 96 well plate, then washed with DPBS and a volume of 200 µL of the H_2DCFDA solution was distributed in each well. Following a 30-minute incubation at 37°C in the dark under a 5% CO_2 atmosphere, cells were washed with DPBS and fluorescence intensity was measured at 485 nm excitation and 535 nm emission wavelengths using a spectrofluorometer Infinite 1000® (TECAN, Neuville-Sur-Oise, France).

2.5. Lipid droplet staining

Cells were seeded on glass slide in 12-well plate at 50,000 cells/well. After a 24-hour exposure to BAK or HO, cells were washed with DPBS and fixed with 4% paraformaldehyde solution in water.

Oil Red O (OR) staining was performed using a 0.5% OR stock solution (Sigma-Aldrich, Saint-Quentin Fallavier, France) diluted to 3/2 (v/v) in distillated water. This solution was distributed in each well. Following a 15-minute incubation, the cells were washed three times in DPBS.

Nile Red (NiR) staining was performed using a stock solution (Thermo Fisher Scientific, Saint-Quentin-Fallavier, France) diluted to 1/1000 (v/v) in a Mowiol® mounting medium. Nuclei were counterstained with DAPI. Glass slides were subsequently mounted under a cover glass in a Mowiol® mounting medium and were observed by epifluorescence microscopy. Quantification of area and size of lipid droplet was performed using imageJ® software (National Institutes of Health).

2.6. Lipidomic analysis

2.6.1. Chemicals and reagents

Chloroform (Carlo Erba Reactifs SDS, Val-de-Reuil, France), acetonitrile, methanol, isopropanol of LC-MS grade (J.T. Baker, Phillipsburg, NJ, USA), 3,5-di-tert-4-butylhydroxytoluene (Sigma Aldrich, Saint-Quentin Fallavier, France) and methyl-tertbutyl-ether (Acros Organics Thermo Fisher Scientific, Villebon-sur-Yvette, France) were used to prepare cell lipid extracts and mobile

phase for reverse phase liquid chromatography. LC-MS grade water (Sigma Aldrich, Saint-Quentin Fallavier, France) was used in sample preparation and analysis. All standard lipids were purchased from Avanti Polar Lipids, Inc. (Alabaster, AL, USA) and are listed in the Table S1 of Supplementary Information.

2.6.2. Sample preparation for lipidomic analysis

Lipidomic analysis was performed as previously described [40,41]. Briefly, cells were harvested using trypsin-EDTA 0.05%, washed with DPBS, centrifuged at 2000 rpm for 10 min. Dry cell pellets were adjusted to 3 million cells and stored at -80°C until analytical process. After thawing, the cell pellets were resuspended in ultra-pure water (1mL) containing a mixture of lipid internal standards (Suppl. Inform. S2) at a final concentration of 1 µM and were sonicated for 5 minutes. Lipids were extracted using a chloroform/methanol/water (5:5:2, v/v/v) mixture containing 3,5-di-tert-4-butylhydroxytoluene 0.01% (w/v) as antioxidant agent. Samples were subsequently centrifuged at 3000 rpm for 10 min, supernatants were collected, and solvents evaporated under reduced pressure at 45 °C. Dry residues were resuspended in an acetonitrile/isopropanol/chloroform/water (35:35:20:10 v/v/v/v) mixture before injection into the UPLC-MS system. Liquid chromatography-electrospray ionization mass spectrometry analysis of lipid extracts was performed on a Synapt®G2 High Definition MS™ (Q-TOF) mass spectrometer (Waters®) combined with a UPLC system (Waters®). Chromatographic separation was performed on an Acquity® CSH C18 column (100× 2.1 mm; 1.7 µm) set at 50°C. Lipids were eluted using a binary gradient system consisting in 10 mM ammonium acetate in an acetonitrile/water mixture (40:60, v/v) as solvent A and 10 mM ammonium acetate in an acetonitrile/isopropanol mixture (10:90, v/v) as solvent B. The eluent increased from 40% B to 100% B in 10 min and was held at 100% B for 2 min before a return to 40% B followed by an equilibration period of 2.5 min. The flow rate was kept at 0.4 mL/min for 15 min. Data were collected in the full scan mode at *m/z* 50–1200 in both positive (ESI +) and negative (ESI−) ion modes. The source parameters were as follows: capillary voltage 3,000 V (ESI +) and 2,400 V (ESI−), cone voltage 30 V (ESI +) and 45 V (ESI−), source temperature 120°C, desolvation temperature 550°C, cone gas flow 20 L/h, and desolvation gas flow 1,000 L/h. Leucine enkephalin (2 ng/mL) was used as the external

reference compound (Lock-Spray™) for mass correction. Data were acquired in the so-called resolution mode (20,000 FWHM a m/z 500) with a scan time of 0.1 s. Data acquisition was managed using Waters MassLynx™ software (version 4.1; Waters MS Technologies).

2.6.3. Data pre-processing

Raw data files (.raw format) acquired on UPLC-ESI-MS were processed using XCMS set up with parameters suitable for high resolution LC-MS, to generate in both ESI+ and ESI-, a matrix listing peak areas associated to a unique *m/z* and retention time. These matrixes were normalized and filtered as previously described [41].

2.6.4. Lipid structure assignment

The structure assignment of lipids was based on the following criteria. An annotation of lipid species was first performed through the use of the online databases LIPID MAPS and METLIN using the mass accuracy with a tolerance window of 5 ppm. The annotation was confirmed using retention time. Indeed, by using the UPLC-ESI-MS analysis of the standard lipid mixture, each lipid class can be determined by the linear relationship between retention time and equivalent carbon number [41]. Finally, MS/MS fragmentation data was used to provide structural information on the annotated lipid structure.

2.6.5. Lipid amount estimation

The lipid quantities, expressed as mol%, were estimated using internal standard lipid mixture spiked in cell suspension samples before extraction, according to procedure in agreement to current guideline [42]. Indeed, lipid species intensities were individually normalized to the one of the corresponding internal standards chosen in the same subclass. The standard lipid mixture includes one lipid species representative of each investigated subclass (Suppl. Inform. S2). Lipid species used as internal standard contain fatty acid side chain with total odd carbon number or are deuteriated derivatives and thus cannot overlap with endogenous lipid species.

2.7. Gene expression analysis by RT-qPCR

Dry cell pellets were stored at -80°C until analysis. Total RNAs were extracted from cells using Nucleospin® RNA kit (Macherey Nagel, Neumann-Neander, Germany). RNA content was measured using a Nanodrop Detector (ND-1000 spectrophotometer, ThermoFischer Scientific). Reverse transcription was performed with 600 ng RNA using Multiscribe reverse transcriptase (TaqMan Reverse Transcription Reagents, Applied Biosystems, Life Technologies). Concentrations of each sample were adjusted to 5 ng/µL of cDNA. The reaction mixture was preheated at 50°C for 2 min, followed by 40 cycles (95°C for 15 s and 60°C for 1 min). Target cDNA was amplified using the 7300 Real-Time PCR system (Applied Biosystems, Life Technologies) with Taqman® probes for *IL1B* (Hs015554136), *IL6* (Hs00174131), *CCL2* (Hs00234140), *CerS2* (Hs00371958), *SMPD2* (Hs00906924), *ASAH2* (HsO1O15655), *DGAT1* (Hs01020362), *PLA1* (Hs01056915) (Thermo Fisher Scientific, Saint-Quentin-Fallavier, France). Each assay was normalized by amplifying the housekeeping cDNA HPRT (Hs02800695). Changes in mRNA expression were calculated according to the $2^{-\Delta\Delta CT}$ method (CT, cycle threshold), with $\Delta CT = CT_{target\ gene} - CT_{HPRT}$ and $\Delta\Delta CT = \Delta CT_{stimulated} - \Delta CT_{control}$.

2.8. PLA_2 activity assay

PLA_2 activity was determined using Red/Green BODIPY based EnzCheck Phospholipase A_2 assay kit according to manufacturer procedure. Briefly, cells were incubated for 24 hours with BAK or HO in 6-well plates. Culture media was removed, and cells were washed with DPBS. Harverest cells were centrifugated, DPBS removed and cell pellet was suspended in 100 µL of PLA_2 reaction buffer with protease inhibitor and finally sonicated for 10 sec. A volume of 50 µL of cell lysate were then transferred in a 96 well plate and mixed with liposomes prepared with the EnzChek Phospholipase A_2 substrate at a ratio of 1:1. Following a 30-minute incubation at 37°C in the dark, PLA_2 activity was determined as a FRET ratio (λ_{ex} = 460 nm λ_{em} = 515/575 nm). Fluorescence were measured using a spectrofluorometer Spark® (TECAN, Neuville-Sur-Oise, France).

2.9. Statistical analysis

Unsupervised and supervised multivariate analyses were performed using SIMCA-P+ software version 13.0.3 (Umetrics, Umeå, Sweden) as previously described [40,41,43]. Briefly, a Pareto scaling was applied to the variables prior to unsupervised principal component analyses (PCA) and supervised partial least squares-discriminant analyses (PLS-DA). Permutation tests on the class labels were conducted to assess over-fitting of models. Orthogonal partial least squares discriminant analyses (OPLS-DA) model was subsequently built based on the corresponding selected PLS-DA models. S-plot was generated from each OPLS-DA model to investigate the lipids involved in the statistically significant differences between control cells and exposed cells. A cross-validated analysis of variance (CV-ANOVA) was carried out on each supervised model to assess the statistical significance of group separation. Finally, a misclassification test was performed to validate the models. Univariate data analysis (Wilcoxon) with a false discovery rate [(FDR)-adjusted $p<0.01$] controlling the false-positive rate associated with multiple comparisons, was performed to assess the whole lipids identified and the statistical significance of the difference in BAK- or HO-treated cells *vs* control cells.

Each experiment was performed independently at least three times. Results are expressed in percentage compared to control and are presented as means ± standard deviation (SD). The statistical analyses were performed using GraphPad Prism 7 software (GraphPad Software, La Jolla, CA). Verification of the normality assumption with an Agostino-Pearson test was first performed. The comparison of the means of more than two groups was then performed using ANOVA test followed by a Dunnet multiple comparison test with a risk set at 0.05. Comparisons of two averages were done using a Student t-test and after normality assessment. The significance thresholds compared to control were: $*p < 0.05$, $**p < 0.01$, $***p < 0.001$.

3. Results

3.1. Cell viability, reactive oxygen species and inflammatory cytokine production following exposure of HCE cells to BAK or HO

Human corneal epithelial cells were exposed for 24 h to BAK concentrations ranging from 10^{-6}% to 10^{-3}% or to HO values ranging from 350 to 600 mOsM respectively. Both BAK and HO led to a significant decrease in viability (data not shown). For subsequent experiments, cells were exposed to 10^{-4}% BAK concentrations, and 500 mOsM HO corresponding to a decrease in viability of 40% ($p < 0.001$), and 35% ($p < 0.001$) (Figure 1A) respectively. A 24-hour exposure of HCE to BAK 10^{-4}% led to a ROS production increase of 190% (Figure 1B). In contrast, HO 500 mOsM did not induce any change in ROS production (Figure 1B). While BAK led to an increase in gene expression of *IL1B* ($p < 0.05$) and *IL6* ($p < 0.01$), HO induced a significant enhancement of the *CCL2* ($p < 0.01$) and *IL6* ($p < 0.001$) gene expressions (Figure 1C).

3.2. Lipid distribution

HO led to the formation of lipid droplets in the cytoplasm of HCE cells (Figure 2A). Indeed, size area (Figure 2B) and number of lipid droplets (Figure 2C) were significantly increased after HO exposure. In contrast, BAK did not induce any change in neutral lipids. It is noteworthy that following HO exposure, the number of LD per HCE cell is lower when staining is performed using Red Oil O than in Red Nil. This discrepancy is related to the fact that droplet fusion specifically occurs in Red Oil O staining protocol [44].

3.3. Changes in lipid composition of HCE cells exposed to BAK or HO

To investigate the impact of BAK or HO exposure on the lipid composition of HCE cells, we performed an untargeted lipidomic analysis using liquid chromatography coupled to mass spectrometry (UPLC-MS). Typical UPLC-ESI-MS in positive (ESI+) and negative (ESI-) ion mode chromatograms of cell lipid extracts from HCE cells are displayed in Figure 3. In positive ion mode, lysophospholipids (LP) and monoacylglycerols (MG) appear between 1.8 and 3 min, phospholipids

(Phosphatidylcholine PC, Phosphatidylethanolamine PE, Phosphatidylinositol PI, phosphatidylglycerol PG and phosphatidylserine PS) and sphingolipids (Sphingomyelin SM and Ceramide Cer) between 5 and 8 min, Diacylgycerol (DG) between 6 and 9 min and Triacylglycerol (TG) between 8 and 11 min. In negative ion mode, fatty acid (FA) are first eluted before 6 min, followed by Cers and phospholipids (PE, PI, PA, PG, and PS) between 6 and 9 min.

Validation of the lipidomic analysis was performed as previously described [40,41]. Briefly, an unsupervised principal component analysis (PCA) was performed based on three quality controls (QCs) dilutions (QC 1/1, 1/3 and 1/6). The built PCA model for the ESI + and ESI- analysis showed compact clusters of replicates for each QC levels ((Suppl. Inform. S1) thus confirming that differences between biological samples were not related to analytical variations.

Unsupervised analysis (PCA) comparing BAK-exposed and control cells was first performed. Both in ESI+ and ESI-, the score plots corresponding to the PCA model which had been created clearly exhibited two clusters ascribed to BAK-exposed and control cells (Figure 3B). The percentage of explained and predicted variances generated exhibited a moderated value for data acquired in ESI+ (R^2 = 0.42, Q^2 = 0.32) and a quite high one for data acquired in ESI- (R^2 = 0.62, Q^2 = 0.52). Unsupervised analysis was also performed to compare the lipidomes of HO-exposed and control cells. Separation between the HO-exposed and control groups was clearly displayed in the score plots (Figure 3B). The percentage of explained and predicted variances generated showed a moderated value for data acquired in ESI+ (R^2 = 0.47, Q^2 = 0.43) and a good one for data acquired in ESI- (R^2 = 0.77, Q^2 = 0.67).

The analysis of the data set corresponding to BAK exposure led to the selection of 1200 variables exhibiting a p(corr) value > 0.7 from the S-Plot (Figure 3C). Among these discriminant variables, 168 were identified as lipids, 120 species were increased and 48 were decreased. Accordingly, exposing HCE cells to BAK led to an increase of sphingolipids including 13 Cer and 10 SM species while 4 hexosylceramides were decreased (Figure 4A). Moreover, the cell level of 17 PC and 14 PE species was significantly decreased while three LPC and two LPE species were enhanced.

295 Finally, seven DG species were decreased, among which three compounds contained saturated or
296 mono-unsaturated fatty acid (Figure 4A).

297 Exposure of HCE cells to 500 mOsM HO made it possible to select 1102 variables with a
298 p(corr) > 0.7 on the corresponding S-Plots (Figure 3C). A total of 132 lipids were identified, 87 lipids
299 being increased and 45 decreased. Results show an increase in sphingolipid species, including 7 Cer
300 and 5 SM (Figure 4). Among glycerophospholipids, only one LPC species decreased while 2 increased
301 and 6 PC and 9 PE increased. Finally, 56 TG species exhibited an increased cell level (Figure 4A).

302 The Venn diagram displayed the lipid species modulated in a common and specific manner
303 following exposure of the HCE cells to BAK or HO (Figure 4B). At the lipid class levels, both BAK
304 and HO respectively increased and decreased the total sphingolipid and phospholipid cell level (Figure
305 4C). In contrast, following exposure of HCE cells to HO, the level of glycerolipids was strikingly
306 increased while fatty acid content was decreased.

307 **3.4. Gene expression and activity of enzymes involved in lipid metabolism**

308 To investigate the origins of the lipidome changes of HCE cells exposed to BAK or HO, we
309 assessed the gene expression of several key enzymes involved in lipid metabolism. Regarding
310 metabolism of sphingolipids (Figure 5A), the total cell level of Cer and SM was increased following
311 exposure to BAK or HO (Figure 5B). The gene expression study showed that *ASAH2*, *CerS2* and
312 *SMPD2* were significantly up regulated after exposure to HO ($p < 0.01$) while incubation with BAK
313 induced no change in expression of these genes (Figure 5C). As total TG cell level was increased
314 following exposure to HO (Figure 6A), enzymes involved in TG biosynthesis (Figure 6B) were also
315 investigated. Results showed an increase in *DGAT1* gene expression ($p < 0.01$) following HO
316 exposure. In contrast, no *DGAT1* modulation was observed after BAK exposure (Figure 6C).
317 Phospholipid metabolism (Figure 7B) was also as BAK and HO induced an increase and a decrease of
318 LPC species, respectively (Figure 7A). Indeed, HO exposure led to an increase in gene expression of
319 *PLA1* ($p < 0.01$) while BAK did not induce such change (Figure 7C). Exposure of HCE cells to BAK

320 and HO induced an increase of PLA2 activity of 35% ($p < 0.05$) and 31% $p < 0.05$), respectively
321 (Figure 7D).

4. Discussion

Dry eye disease is a chronic inflammatory pathology of the ocular surface with significant impact on everyday life for patients. Despite its high prevalence, only few treatments are available. It is thus important to better understand molecular mechanisms of the pathology in order to develop new targeted treatments and to find new markers to improve patient monitoring. Lipids are now recognized as mediators of the signal transduction with molecular impact on cell homeostasis and with an important role in inflammatory process. Our purpose was therefore to investigate the lipid changes in an *in vitro* model of human epithelial corneal cell line, exposed to BAK or hyperosmolarity (HO). These both cell stress, HO, key feature in the pathophysiology of DED and BAK, common eye drop excipient, are known to be contributing factor of this eye disease [9].

BAK concentration and HO value were chosen according to eye drop concentration for BAK and HO value determinated in the context of DED and also using HCE cell viability assays and previously published reports. Indeed, a 24-hour exposure to BAK 10^{-4}% or HO 500 mOsM leads to a significant decrease in cell viability associated to an increase in gene expression of pro-inflammatory cytokines as previously described in DED patients [45,46]. Our results are in accordance with previous studies investigating BAK and HO [20,47,48]. It must be emphasized, that the aforementioned BAK concentration is 1/50 to 1/200 times that used in commercially available eye-drops (0.005% – 0.02%). Regarding HO, in DED patients, mean HO levels range from 310 to 330 mOsM [5] and values up to 800 mOsM have been previously reported in tears of DED patients [49]. In addition, a HO level of 500 mOsM has been widely used in *in vitro* models of DED [21,23,24,50].

In order to exhaustively list the lipid species which level is modified following BAK or HO exposure in HCE, we performed an untargeted lipidomic analysis involving UPLC-ESI-HRMS as well as supervised and unsupervised multivariate analyses. Indeed, this analytical approach is recognized to be able to extensively characterize qualitative and quantitative changes in lipid composition without *a priori*, especially in cells [40,51]. In HCE incubated either to BAK 10^{-4}% or to HO 500 mOsM, three main lipid classes display marked alterations: sphingolipids, glycerolipids and glycerophospholipids.

In HCE exposed to BAK or HO, a major change in sphingolipid level was observed. Changes involving this lipid subclass was previously reported in a 3D-reconstructed human-cornea-like epithelium exposed to 0.1% BAK and in a human corneal cell line exposed to HO [52,53]. In our study, both BAK and HO also increased ceramide species levels, especially Cer (44:2), Cer (42:2), Cer (36:2) and Cer (34:1). HO mainly increased long chain ceramides. This result is consistent with an increase in gene expression of CerS2 also only confirmed in HCE cells exposed to HO. Indeed, CerS2 catalyzes acetylation of sphinganine or sphingosine by C20 to C26 fatty acid to form dihydroceramides and ceramides, respectively [26]. In contrast, BAK mainly increasing short chain ceramides is therefore not expected to change in CerS2 gene expression. It would be of interest to investigate gene expression of *CerS6*, an enzyme specifically catalyzing short chain ceramide biosynthesis. Beside *de novo* synthesis, ceramides are produced through the cleavage of sphingomyelins by sphingomyelinase enzymes. *nSMase2* gene expression was increased following HO exposure, suggesting that ceramide accumulation could be due to sphingomyelin hydrolysis, as previously reported after a 2 hour-HO exposure in corneal cells [52]. Metabolism of ceramides also includes degradation into sphingosines via a ceramidase, especially ASAH2, an enzyme whose gene exhibited an increased expression in HCE exposed to HO. Mechanisms of Cer accumulation involve different metabolic pathways related to specific cell locations. On one hand, de novo synthesis of ceramides take place in the endoplasmic reticulum and involves enzymes such as serine palmitotoyl transferase and ceramide synthase. On the other hand, the hydrolysis of SM into Cer can be achieved at the plasma membrane by neutral SMase but also in lysosomes by acid SMase. In dry eye disease models, a global profiling of the enzymes involved in the synthesis of ceramides could be of particular interest to target one or more enzymes to be investigated in subsequent pharmacological studies.

Ceramides promote inflammation through IL-1β release, induce apoptosis and alter cell survival through PKCζ and PP2A activation [27,54,55]. Ceramides thus play key roles in various cell processes, and the dysregulation of ceramide metabolism is involved in many inflammatory diseases such as atherosclerosis, inflammatory bowel disease or multiple sclerosis [28,56,57]. Our results show that HO leads to an increase in both *CerS2* and *CCL2* gene expression. On one hand, *de novo* synthesis

of ceramide was shown to induce a CCL2 release in a macrophage cell line [58] and on the other hand, HO is a well-known inducer of CCL2, stimulating gene expression and protein release [22,24,48]. *De novo* synthesis of ceramide may thus stimulate CCL2 release leading to the recruitment of macrophages which, in turn, triggers inflammatory pathways. In contrast to HO, incubation with BAK did not modify CerS2 and CCL2 gene expression in HCE.

The increase in ceramide levels, described in our study, following a 24-hour incubation of HCE with BAK or HO, previously reported by Robciuc et al. but following a shorter exposure of 2 hours, indicates effect during at least 24 hours. In a short time exposure, Cer is produced through the action of SMase, a well-known mechanism occurring in the acute phase of apoptosis, while our study indicates that following a 24-hours exposure, de novo synthesis pathway is also involved. Regarding apoptosis and inflammatory process induced by this lipid subclass [59], ceramides may be regarded as important mediators of the deleterious effects due to HO or BAK.

The present untargeted lipidomic analysis indicates a striking increase in TG species induced by HO exposure. This result is supported by lipid droplet (LD) formation and by *DGAT1* gene overexpression in the HCE cells. HO is known to induce LD formation in renal as well as corneal epithelial cells [52,60] and DGAT1 is one of the main enzymes involved in TG biosynthesis. LD are an active field of research because their role has been described as either protective or deleterious [61,62]. Indeed, LD are involved in free fatty acids storage playing a protective role against cell lipotoxicity [62,63]. However, LD are also known to be deleterious to cells as they are key effectors of inflammation [64], especially through the COX2 activity, an enzyme located in LD catalyzing synthesis of pro-inflammatory eicosanoids [64]. We may thus hypothesize that HO leads to eicosanoid formation. A target lipidomic analysis would therefore be valuable to assess eicosanoid level changes after BAK and HO exposure. In consistency with our results, an increase in COX2 protein was reported in primary epithelial corneal cells and in a conjunctival cell line after HO exposure [21,65]. LD could therefore be explored as a cell marker of hyperosmolarity of the ocular surface.

In vitro BAK exposure led to both a striking decrease in PC and PE associated to an increase in LPC and LPE. These results are in complete agreement with the increase of PLA_2 activity, the enzyme responsible for the sn_2 acyl chain hydrolysis of phospholipids. Furthermore, an important decrease in PC-O (36:4) level which contain arachidonic acid in sn_2 position was especially observed. This result may be expected since PC containing arachidonic acid in sn_2 position is a key substrate of PLA_2 enzyme. As PUFA are mainly targeted by PLA_2, the decrease in PC (O-18:0/22:6) level may also be related to the increase of DHA rate which could constitute a cell response against BAK exposure. As an increase of PLA_2 has been previously reported in tears of DED patients [66], this enzyme could thus promote BAK toxicity in human corneal epithelial cells. Indeed, it was demonstrated that in a macrophage cell line, LPC promote inflammation through IL-6 and TNFα release [67,68]. In addition, *in vitro*, LPC triggers signaling pathways of TLR-4, a major lipopolysaccharide pattern recognition receptor widely described in DED pathophysiology [2,69,70]. LPC may thus contribute to inflammation mediated by BAK and hence, play a role in its toxicity.

In contrast, HO exposure induced a marked increase in PE levels. A similar change has been previously described in renal cells exposed to HO [60]. A slight decrease in LPC levels associated to an increase in *PLA1* gene expression was also exhibited. PLA_1 catalyzes LPC conversion to glycerylphosphorylcholines, known to be osmoprotective compounds. Our results are compatible with the previously reported increase in glycerylphosphorylcholine level in the IOBA-NHC conjunctival cell line exposed to HO [65]. Furthermore, a metabolomic study on DED patient serum exhibited glycerylphosphorylcholine and lysolipid changes [71] indicating an alteration of this lipid subclass, in consistency with our results. Increase in catabolism of PC may thus be regarded as a self-protective mechanism of cells to osmotic stress via osmoprotective glycerylphosphorylcholine [72].

In addition, numerous PC, PE and PI plasmalogen species are strikingly decreased in HCE cells under BAK or HO exposure. This result may be explained by the fact that vinyl ether located in sn_1 position is very sensitive to oxidative stress [73,74]. Oxidative stress is known to be part of the mechanisms explaining deleterious effect observed under BAK and HO exposure [20,75,76]. An

increase in ROS production observed in HCE cells following a 24-hour exposure of BAK reinforced the above observations. In contrast, HO exposure did not lead to any ROS production after 24 hours. Nevertheless, it has been shown that HO lead to oxidative stress but only following 1 to 3 hours exposure [21]. Regarding oxidative stress in DED pathophysioplogy, plasmalogen species may finally be regarded as cell marker.

In summary, exposure of HCE to BAK or HO highlights a large set of lipid mediator modulation. Interestingly, these two *in vitro* models showed common and specific alterations in the cell lipidome. An overview of major lipid alterations reported in this study is displayed in the Figure 8. While ceramides were increased both after BAK or HO exposure, changes in glycerolipids and phospholipids depend on the type of the stressor involved. Indeed, TG accumulation and LD formation were specifically induced by HO while a slight TG decrease arouse following BAK exposure. Moreover, LPE and LPC drastically decreased following HO exposure, while BAK induces an increase in these two lipid subclasses. Using epithelial corneal cells exposed to BAK, a microbicidal, detergent and pro-oxidative agent, or HO, a pathophysiological feature of DED, this untargeted lipidomic investigation showed common and contrasted cell lipid alterations. It also underlines the weight of lipid metabolism in cell death and inflammation processes. Finally, all the impacted lipid species could be tightly intricated in a metabolic network underlying specific regulation pathways in addition to other biological processes.

5. Conclusion

From a clinical point of view, the lipid changes specific to BAK or HO observed with this human corneal cell line provide new insights in DED diagnosis. Our study also highlights alterations in the metabolism of sphingolipids, an important bioactive lipid class involved in inflammatory processes, thus opening a new way to consider their role in the DED pathophysiology. Moreover, this study provides new perspectives in the research of biomarkers and therapeutic targets involving cellular lipids in DED.

Aknowledgment

This study was funded by Sorbonne Université and the Institut National de la Santé et de la Recherche Médicale and Centre National de la Recherche Scientifique. The authors thank the core facilities of the Institut de la vision, the Centre Hospitalier National d'Ophtalmologie des Quinze-Vingts, Région Ile-de-France and Ville de Paris.

Conflict of interest

The authors declare that they have no conflicts of interest.

References

[1] F. Stapleton, M. Alves, V.Y. Bunya, I. Jalbert, K. Lekhanont, F. Malet, K.-S. Na, D. Schaumberg, M. Uchino, J. Vehof, E. Viso, S. Vitale, L. Jones, TFOS DEWS II Epidemiology Report, Ocul. Surf. 15 (2017) 334–365. doi:10.1016/j.jtos.2017.05.003.

[2] J.P. Craig, K.K. Nichols, E.K. Akpek, B. Caffery, H.S. Dua, C. Joo, Z. Liu, J.D. Nelson, J.J. Nichols, K. Tsubota, F. Stapleton, The Ocular Surface TFOS DEWS II De fi nition and Classi fi cation Report, 15 (2017) 276–283. doi:10.1016/j.jtos.2017.05.008.

[3] M.L. Massingale, X. Li, M. Vallabhajosyula, D. Chen, Y. Wei, P.A. Asbell, Analysis of inflammatory cytokines in the tears of dry eye patients, Cornea. 28 (2009) 1023–1027. doi:10.1097/ICO.0b013e3181a16578.

[4] K.S. Na, J.W. Mok, J.Y. Kim, C.R. Rho, C.K. Joo, Correlations between tear cytokines, chemokines, and soluble receptors and clinical severity of dry eye disease, Investig. Ophthalmol. Vis. Sci. 53 (2012) 5443–5450. doi:10.1167/iovs.11-9417.

[5] C. Baudouin, P. Aragona, E.M. Messmer, A. Tomlinson, M. Calonge, K.G. Boboridis, Y.A. Akova, G. Geerling, M. Labetoulle, M. Rolando, Role of hyperosmolarity in the pathogenesis and management of dry eye disease: Proceedings of the ocean group meeting, Ocul. Surf. 11 (2013) 246–258. doi:10.1016/j.jtos.2013.07.003.

[6] S.C. Pflugfelder, C.S. de Paiva, The Pathophysiology of Dry Eye Disease: What We Know and Future Directions for Research, Ophthalmology. 124 (2017) S4–S13. doi:10.1016/j.ophtha.2017.07.010.

[7] M.K. Rhee, F.S. Mah, Inflammation in Dry Eye Disease, Ophthalmology. 124 (2017) S14–S19. doi:10.1016/j.ophtha.2017.08.029.

[8] J.A.P. Gomes, D.T. Azar, C. Baudouin, N. Efron, M. Hirayama, J. Horwath-Winter, T. Kim, J.S. Mehta, E.M. Messmer, J.S. Pepose, V.S. Sangwan, A.L. Weiner, S.E. Wilson, J.S. Wolffsohn, TFOS DEWS II iatrogenic report, Ocul. Surf. 15 (2017) 511–538. doi:10.1016/j.jtos.2017.05.004.

[9] C. Baudouin, A. Labbé, H. Liang, A. Pauly, F. Brignole-Baudouin, Preservatives in eyedrops: The good, the bad and the ugly, Prog. Retin. Eye Res. 29 (2010) 312–334. doi:10.1016/j.preteyeres.2010.03.001.

[10] F. Ferk, M. Mišik, C. Hoelzl, M. Uhl, M. Fuerhacker, B. Grillitsch, W. Parzefall, A. Nersesyan, K. Mičieta, T. Grummt, V. Ehrlich, S. Knasmüller, Benzalkonium chloride (BAC) and dimethyldioctadecyl-ammonium bromide (DDAB), two common quaternary ammonium

compounds, cause genotoxic effects in mammalian and plant cells at environmentally relevant concentrations, Mutagenesis. 22 (2007) 363–370. doi:10.1093/mutage/gem027.

[11] C.A. Rasmussen, P.L. Kaufman, J.A. Kiland, Benzalkonium Chloride and Glaucoma, J. Ocul. Pharmacol. Ther. 30 (2014) 163–169. doi:10.1089/jop.2013.0174.

[12] D. Vaede, C. Baudouin, J.M. Warnet, F. Brignole-Baudouin, Les conservateurs des collyres: Vers une prise de conscience de leur toxicité, J. Fr. Ophtalmol. 33 (2010) 505–524. doi:10.1016/j.jfo.2010.06.018.

[13] F. Brignole-Baudouin, N. Desbenoit, G. Hamm, H. Liang, J.P. Both, A. Brunelle, I. Fournier, V. Guerineau, R. Legouffe, J. Stauber, D. Touboul, M. Wisztorski, M. Salzet, O. Laprevote, C. Baudouin, A New Safety Concern for Glaucoma Treatment Demonstrated by Mass Spectrometry Imaging of Benzalkonium Chloride Distribution in the Eye, an Experimental Study in Rabbits, PLoS One. 7 (2012). doi:10.1371/journal.pone.0050180.

[14] A.M. Stevens, P.A. Kestelyn, D. De Bacquer, P.G. Kestelyn, Benzalkonium chloride induces anterior chamber inflammation in previously untreated patients with ocular hypertension as measured by flare meter: A randomized clinical trial, Acta Ophthalmol. 90 (2012) 221–224. doi:10.1111/j.1755-3768.2011.02338.x.

[15] A.A. Bonniard, J.Y. Yeung, C.C. Chan, C.M. Birt, A. Aguayo, J.Y. Yeung, C.C. Chan, C.M. Birt, Expert Opinion on Drug Metabolism & Toxicology Ocular surface toxicity from glaucoma topical medications and associated preservatives such as benzalkonium chloride (BAK), 5255 (2016). doi:10.1080/17425255.2016.1209481.

[16] C. Baudouin, M. Irkeç, E.M. Messmer, J.M. Benítez-del-Castillo, S. Bonini, F.C. Figueiredo, G. Geerling, M. Labetoulle, M. Lemp, M. Rolando, G. Van Setten, P. Aragona, ODISSEY European Consensus Group Members, Clinical impact of inflammation in dry eye disease: proceedings of the ODISSEY group meeting, Acta Ophthalmol. 96 (2018) 111–119. doi:10.1111/aos.13436.

[17] W. Stevenson, S.K. Chauhan, R. Dana, Dry Eye Disease, Arch. Ophthalmol. 130 (2012) 90. doi:10.1001/archophthalmol.2011.364.

[18] M. De Saint Jean, C. Debbasch, F. Brignole, P. Rat, J.M. Warnet, C. Baudouin, Toxicity of preserved and unpreserved antiglaucoma topical drugs in an in vitro model of conjunctival cells., Curr. Eye Res. 20 (2000) 85–94. doi:10.176/0271-3683(200002)20:2;1-d;ft085.

[19] D.-Q. Li, Z. Chen, X.J. Song, L. Luo, S.C. Pflugfelder, Stimulation of matrix metalloproteinases by hyperosmolarity via a JNK pathway in human corneal epithelial cells., Invest. Ophthalmol. Vis. Sci. 45 (2004) 4302–11. doi:10.1167/iovs.04-0299.

[20] C. Clouzeau, D. Godefroy, L. Riancho, W. Rostène, C. Baudouin, F. Brignole-Baudouin, Hyperosmolarity potentiates toxic effects of benzalkonium chloride on conjunctival epithelial cells in vitro., Mol. Vis. 18 (2012) 851–63.

[21] R. Deng, X. Hua, J. Li, W. Chi, Z. Zhang, F. Lu, L. Zhang, S.C. Pflugfelder, D.-Q. Li, Oxidative stress markers induced by hyperosmolarity in primary human corneal epithelial cells., PLoS One. 10 (2015) e0126561. doi:10.1371/journal.pone.0126561.

[22] E. Warcoin, C. Baudouin, C. Gard, F. Brignole-Baudouin, In Vitro Inhibition of NFAT5-Mediated Induction of CCL2 in Hyperosmotic Conditions by Cyclosporine and Dexamethasone on Human HeLa-Modified Conjunctiva-Derived Cells, PLoS One. 11 (2016) e0159983. doi:10.1371/journal.pone.0159983.

[23] M.E. Cavet, K.L. Harrington, T.R. Vollmer, K.W. Ward, J.-Z. Zhang, Anti-inflammatory and anti-oxidative effects of the green tea polyphenol epigallocatechin gallate in human corneal epithelial cells., Mol. Vis. 17 (2011) 533–42. http://www.pubmedcentral.nih.gov/articlerender.fcgi?artid=3044696&tool=pmcentrez&rendertype=abstract.

[24] X. Hua, R. Deng, J. Li, W. Chi, Z. Su, J. Lin, S. Pflugfelder, D. Li, Protective Effects of L-Carnitine Against Oxidative Injury by Hyperosmolarity in Human Corneal Epithelial Cells, Invest. Ophthalmol. Vis. Sci. 56 (2015) 5503–11.

[25] L. Magtanong, P.J. Ko, S.J. Dixon, Emerging roles for lipids in non-apoptotic cell death, Cell Death Differ. 23 (2016) 1099–1109. doi:10.1038/cdd.2016.25.

[26] S. Grösch, S. Schiffmann, G. Geisslinger, Progress in Lipid Research Chain length-specific properties of ceramides, 51 (2012) 50–62. doi:10.1016/j.plipres.2011.11.001.

[27] B.J. Pettus, C.E. Chalfant, Y.A. Hannun, Ceramide in apoptosis: an overview and current perspectives, Biochim. Biophys. Acta - Mol. Cell Biol. Lipids. 1585 (2002) 114–125. doi:10.1016/S1388-1981(02)00331-1.

[28] J. Kurz, M.J. Parnham, G. Geisslinger, S. Schiffmann, Ceramides as Novel Disease Biomarkers., Trends Mol. Med. 25 (2019) 20–32. doi:10.1016/j.molmed.2018.10.009.

[29] Y.A. Hannun, L.M. Obeid, Principles of bioactive lipid signalling: Lessons from sphingolipids, Nat. Rev. Mol. Cell Biol. 9 (2008) 139–150. doi:10.1038/nrm2329.

[30] S. Priyadarsini, A. Sarker-Nag, J. Allegood, C. Chalfant, D. Karamichos, Description of the sphingolipid content and subspecies in the diabetic cornea., Curr. Eye Res. 40 (2015) 1204–10. doi:10.3109/02713683.2014.990984.

[31] A. Robciuc, T. Hyötyläinen, M. Jauhiainen, J.M. Holopainen, Ceramides in the Pathophysiology of the Anterior Segment of the Eye, Curr. Eye Res. 38 (2013) 1006–1016. doi:10.3109/02713683.2013.810273.

[32] B.M. Ham, J.T. Jacob, M.M. Keese, R.B. Cole, Identification, quantification and comparison of major non-polar lipids in normal and dry eye tear lipidomes by electrospray tandem mass spectrometry., J. Mass Spectrom. 39 (2004) 1321–36. doi:10.1002/jms.725.

[33] S.M. Lam, L. Tong, B. Reux, X. Duan, A. Petznick, S.S. Yong, C.B.S. Khee, M.J. Lear, M.R. Wenk, G. Shui, Lipidomic analysis of human tear fluid reveals structure-specific lipid alterations in dry eye syndrome., J. Lipid Res. 55 (2014) 299–306. doi:10.1194/jlr.P041780.

[34] Y.A. Ambaw, C. Chao, S. Ji, M. Raida, F. Torta, M.R. Wenk, L. Tong, Tear eicosanoids in healthy people and ocular surface disease., Sci. Rep. 8 (2018) 11296. doi:10.1038/s41598-018-29568-3.

[35] J. Chen, K.K. Nichols, L. Wilson, S. Barnes, J.J. Nichols, Untargeted lipidomic analysis of human tears: A new approach for quantification of O-acyl-omega hydroxy fatty acids., Ocul. Surf. 17 (2019) 347–355. doi:10.1016/j.jtos.2019.02.004.

[36] E. Warcoin, C. Clouzeau, F. Brignole-Baudouin, C. Baudouin, Hyperosmolarité : effets intracellulaires et implication dans la sécheresse oculaire, J. Fr. Ophtalmol. 39 (2016) 641–651. doi:10.1016/j.jfo.2016.07.006.

[37] S.-W. Chang, R.-F. Chi, C.-C. Wu, M.-J. Su, Benzalkonium Chloride and Gentamicin Cause a Leak in Corneal Epithelial Cell Membrane, Exp. Eye Res. 71 (2000) 3–10. doi:10.1006/exer.2000.0849.

[38] K. Araki-Sasaki, Y. Ohashi, T. Sasabe, K. Hayashi, H. Watanabe, Y. Tano, H. Handa, An SV40-immortalized human corneal epithelial cell line and its characterization., Invest. Ophthalmol. Vis. Sci. 36 (1995) 614–21. http://www.ncbi.nlm.nih.gov/pubmed/7534282.

[39] G. Repetto, A. del Peso, J.L. Zurita, Neutral red uptake assay for the estimation of cell viability/cytotoxicity., Nat. Protoc. 3 (2008) 1125–31. doi:10.1038/nprot.2008.75.

[40] J. Petit, A. Wakx, S. Gil, T. Fournier, N. Auzeil, P. Rat, O. Laprévote, Lipidome-wide disturbances of human placental JEG-3 cells by the presence of MEHP., Biochimie. 149 (2018) 1–8. doi:10.1016/j.biochi.2018.03.002.

[41] J. Lanzini, D. Dargère, A. Regazzetti, A. Tebani, O. Laprévote, N. Auzeil, Changing in lipid profile induced by the mutation of Foxn1 gene: A lipidomic analysis of Nude mice skin, Biochimie. 118 (2015) 234–243. doi:10.1016/j.biochi.2015.09.029.

[42] B. Burla, M. Arita, M. Arita, A.K. Bendt, A. Cazenave-Gassiot, E.A. Dennis, K. Ekroos, X. Han, K. Ikeda, G. Liebisch, M.K. Lin, T.P. Loh, P.J. Meikle, M. Orešič, O. Quehenberger, A. Shevchenko, F. Torta, M.J.O. Wakelam, C.E. Wheelock, M.R. Wenk, MS-based lipidomics of human blood plasma: a community-initiated position paper to develop accepted guidelines., J. Lipid Res. 59 (2018) 2001–2017. doi:10.1194/jlr.S087163.

[43] S. Ayciriex, F. Djelti, S. Alves, A. Regazzetti, M. Gaudin, J. Varin, D. Langui, I. Bièche, E. Hudry, D. Dargère, P. Aubourg, N. Auzeil, O. Laprévote, N. Cartier, Neuronal Cholesterol Accumulation Induced by Cyp46a1 Down-Regulation in Mouse Hippocampus Disrupts Brain Lipid Homeostasis, Front. Mol. Neurosci. 10 (2017) 211. doi:10.3389/fnmol.2017.00211.

[44] S. Fukumoto, T. Fujimoto, Deformation of lipid droplets in fixed samples, Histochem. Cell Biol. 118 (2002) 423–428. doi:10.1007/s00418-002-0462-7.

[45] H. Liang, K. Kessal, G. Rabut, P. Daull, J.S. Garrigue, S. Melik Parsadaniantz, M. Docquier, C. Baudouin, F. Brignole-Baudouin, Correlation of clinical symptoms and signs with conjunctival gene expression in primary Sjögren syndrome dry eye patients., Ocul. Surf. (2019). doi:10.1016/j.jtos.2019.03.005.

[46] K. Kessal, H. Liang, G. Rabut, P. Daull, J.-S. Garrigue, M. Docquier, S. Melik Parsadaniantz, C. Baudouin, F. Brignole-Baudouin, Conjunctival Inflammatory Gene Expression Profiling in Dry Eye Disease: Correlations With HLA-DRA and HLA-DRB1., Front. Immunol. 9 (2018) 2271. doi:10.3389/fimmu.2018.02271.

[47] E. Brasnu, F. Brignole-Baudouin, L. Riancho, J.-M. Warnet, C. Baudouin, Comparative study on the cytotoxic effects of benzalkonium chloride on the Wong-Kilbourne derivative of Chang conjunctival and IOBA-NHC cell lines., Mol. Vis. 14 (2008) 394–402. http://www.ncbi.nlm.nih.gov/pubmed/18334956%0Ahttp://www.pubmedcentral.nih.gov/articlerender.fcgi?artid=PMC2268853.

[48] E. Warcoin, C. Clouzeau, C. Roubeix, A.L. Raveu, D. Godefroy, L. Riancho, C. Baudouin, F. Brignole-Baudouin, Hyperosmolarity and Benzalkonium Chloride Differently Stimulate Inflammatory Markers in Conjunctiva-Derived Epithelial Cells in vitro, Ophthalmic Res. 58 (2017) 40–48. doi:10.1159/000448117.

[49] H. Liu, C. Begley, M. Chen, A. Bradley, J. Bonanno, N.A. McNamara, J.D. Nelson, T. Simpson, A Link between Tear Instability and Hyperosmolarity in Dry Eye, Investig. Opthalmology Vis. Sci. 50 (2009) 3671. doi:10.1167/iovs.08-2689.

[50] Y. Ren, H. Lu, P.S. Reinach, Q. Zheng, J. Li, Q. Tan, H. Zhu, W. Chen, Hyperosmolarity-induced AQP5 upregulation promotes inflammation and cell death via JNK1/2 Activation in

human corneal epithelial cells, Sci. Rep. 7 (2017) 1–11. doi:10.1038/s41598-017-05145-y.

[51] E. Saunier, S. Antonio, A. Regazzetti, N. Auzeil, O. Laprévote, J.W. Shay, X. Coumoul, R. Barouki, C. Benelli, L. Huc, S. Bortoli, Resveratrol reverses the Warburg effect by targeting the pyruvate dehydrogenase complex in colon cancer cells., Sci. Rep. 7 (2017) 6945. doi:10.1038/s41598-017-07006-0.

[52] A. Robciuc, T. Hyötyläinen, M. Jauhiainen, J.M. Holopainen, Hyperosmolarity-induced lipid droplet formation depends on ceramide production by neutral sphingomyelinase 2, J. Lipid Res. 53 (2012) 2286–2295. doi:10.1194/jlr.M026732.

[53] M. Lee, K.M. Joo, S. Choi, S.H. Lee, S.Y. Kim, Y.J. Chun, D. Choi, K.M. Lim, Nervonoylceramide (C24:1Cer), a lipid biomarker for ocular irritants released from the 3D reconstructed human cornea-like epithelium, MCTT HCE™, Toxicol. Vitr. 47 (2018) 94–102. doi:10.1016/j.tiv.2017.11.008.

[54] M. Maceyka, S. Spiegel, Sphingolipid metabolites in inflammatory disease, Nature. 510 (2014) 58–67. doi:10.1038/nature13475.

[55] B. Chaurasia, S.A. Summers, Ceramides – Lipotoxic Inducers of Metabolic Disorders, Trends Endocrinol. Metab. 26 (2015) 538–550. doi:10.1016/j.tem.2015.07.006.

[56] J.L. Stith, F.N. Velazquez, L.M. Obeid, Advances in determining signaling mechanisms of ceramide and role in disease, J. Lipid Res. 60 (2019) 913–918. doi:10.1194/jlr.s092874.

[57] J.-W. Park, W.-J. Park, A.H. Futerman, Ceramide synthases as potential targets for therapeutic intervention in human diseases, Biochim. Biophys. Acta - Mol. Cell Biol. Lipids. 1841 (2014) 671–681. doi:10.1016/J.BBALIP.2013.08.019.

[58] Y. Hamada, H. Nagasaki, A. Fujiya, Y. Seino, Q.L. Shang, T. Suzuki, H. Hashimoto, Y. Oiso, Involvement of de novo ceramide synthesis in pro-inflammatory adipokine secretion and adipocyte-macrophage interaction, J. Nutr. Biochem. 25 (2014) 1309–1316. doi:10.1016/j.jnutbio.2014.07.008.

[59] R.A. Claus, M.J. Dorer, A.C. Bunck, H.P. Deigner, Inhibition of sphingomyelin hydrolysis: targeting the lipid mediator ceramide as a key regulator of cellular fate., Curr. Med. Chem. 16 (2009) 1978–2000. http://www.ncbi.nlm.nih.gov/pubmed/19519377.

[60] K. Weber, C. Casali, V. Gaveglio, S. Pasquaré, E. Morel Gómez, L. Parra, L. Erjavec, C. Perazzo, M.C. Fernández Tome, TAG synthesis and storage under osmotic stress. A requirement for preserving membrane homeostasis in renal cells, Biochim. Biophys. Acta - Mol. Cell Biol. Lipids. 1863 (2018) 1108–1120. doi:10.1016/j.bbalip.2018.06.012.

652 [61] M.A. Welte, A.P. Gould, Lipid droplet functions beyond energy storage, Biochim. Biophys.
653 Acta - Mol. Cell Biol. Lipids. 1862 (2017) 1260–1272. doi:10.1016/j.bbalip.2017.07.006.

654 [62] A.R. Thiam, R. V. Farese, T.C. Walther, The biophysics and cell biology of lipid droplets, Nat.
655 Rev. Mol. Cell Biol. 14 (2013) 775–786. doi:10.1038/nrm3699.

656 [63] M.A. Welte, Expanding Roles for Lipid Droplets, Curr. Biol. 25 (2015) R470–R481.
657 doi:10.1016/j.cub.2015.04.004.

658 [64] S. Xu, X. Zhang, P. Liu, Lipid droplet proteins and metabolic diseases, Biochim. Biophys. Acta
659 - Mol. Basis Dis. 1864 (2018) 1968–1983. doi:10.1016/j.bbadis.2017.07.019.

660 [65] L. Chen, J. Li, T. Guo, S. Ghosh, S.K. Koh, D. Tian, L. Zhang, D. Jia, R.W. Beuerman, R.
661 Aebersold, E.C.Y. Chan, L. Zhou, Global Metabonomic and Proteomic Analysis of Human
662 Conjunctival Epithelial Cells (IOBA-NHC) in Response to Hyperosmotic Stress, J. Proteome
663 Res. 14 (2015) 3982–3995. doi:10.1021/acs.jproteome.5b00443.

664 [66] D. Chen, Y. Wei, X. Li, S. Epstein, J.M. Wolosin, P. Asbell, sPLA2-IIa is an inflammatory
665 mediator when the ocular surface is compromised., Exp. Eye Res. 88 (2009) 880–8.
666 doi:10.1016/j.exer.2008.11.035.

667 [67] I. Sevastou, E. Kaffe, M.-A. Mouratis, V. Aidinis, Lysoglycerophospholipids in chronic
668 inflammatory disorders: The PLA2/LPC and ATX/LPA axes, Biochim. Biophys. Acta - Mol.
669 Cell Biol. Lipids. 1831 (2013) 42–60. doi:10.1016/j.bbalip.2012.07.019.

670 [68] J. Chen, X. Cao, Y. Cui, G. Zeng, J. Chen, G. Zhang, Resveratrol alleviates
671 lysophosphatidylcholine-induced damage and inflammation in vascular endothelial cells, Mol.
672 Med. Rep. (2017). doi:10.3892/mmr.2017.8300.

673 [69] R.L. Redfern, S. Barabino, J. Baxter, C. Lema, A.M. McDermott, Dry eye modulates the
674 expression of toll-like receptors on the ocular surface, Exp. Eye Res. 134 (2015) 80–89.
675 doi:10.1016/j.exer.2015.03.018.

676 [70] H.S. Lee, T. Hattori, E.Y. Park, W. Stevenson, S.K. Chauhan, R. Dana, Expression of toll-like
677 receptor 4 contributes to corneal inflammation in experimental dry eye disease., Invest.
678 Ophthalmol. Vis. Sci. 53 (2012) 5632–40. doi:10.1167/iovs.12-9547.

679 [71] J. Vehof, P.G. Hysi, C.J. Hammond, A Metabolome-Wide Study of Dry Eye Disease Reveals
680 Serum Androgens as Biomarkers, Ophthalmology. 124 (2017) 505–511.
681 doi:10.1016/j.ophtha.2016.12.011.

682 [72] M. Gallazzini, M.B. Burg, What's New About Osmotic Regulation of Glycerophosphocholine,
683 Physiology. 24 (2009) 245–249. doi:10.1152/physiol.00009.2009.

[73] N.E. Braverman, A.B. Moser, Functions of plasmalogen lipids in health and disease, Biochim. Biophys. Acta - Mol. Basis Dis. 1822 (2012) 1442–1452. doi:10.1016/J.BBADIS.2012.05.008.

[74] S. Wallner, G. Schmitz, Plasmalogens the neglected regulatory and scavenging lipid species, Chem. Phys. Lipids. 164 (2011) 573–589. doi:10.1016/j.chemphyslip.2011.06.008.

[75] T. Pauloin, M. Dutot, J.-M. Warnet, P. Rat, In vitro modulation of preservative toxicity: High molecular weight hyaluronan decreases apoptosis and oxidative stress induced by benzalkonium chloride, Eur. J. Pharm. Sci. 34 (2008) 263–273. doi:10.1016/j.ejps.2008.04.006.

[76] M.-A. Vitoux, K. Kessal, S. Melik Parsadaniantz, M. Claret, C. Guerin, C. Baudouin, F. Brignole-Baudouin, A. Réaux-Le Goazigo, Benzalkonium chloride-induced direct and indirect toxicity on corneal epithelial and trigeminal neuronal cells: proinflammatory and apoptotic responses in vitro, Toxicol. Lett. 319 (2020) 74–84. doi:10.1016/J.TOXLET.2019.10.014.

Figures

Figure 1: Effects of BAK or HO on corneal epithelial cells viability. Viability (A) and reactive oxygen species (B) assay were performed following a 24-hour exposure to BAK or hyperosmolarity. Markers of inflammation (C) were assessed by RT-qPCR for both exposures. Results are expressed as mean ± SD of fold change compared of control (ANOVA with Tukey's multiple comparisons test. n=4. *$p < 0.05$; **$p < 0.01$; ***$p < 0.001$).

Figure 2: Lipid staining following BAK or HO exposure. HO induces lipid droplet formation (A) in the cytoplasm of HCE cells with an increase of their size and area (B). Results are expressed as mean ± SD (ANOVA with Tukey's multiple comparisons test. n=4. *$p < 0.05$; **$p < 0.01$; ***$p < 0.001$).

Figure 3: Liquid chromatography time-of-flight mass spectrometry-based lipidomics analysis following BAK or HO exposure. Chromatograms (A) and PCA built models (B) of control and exposed HCE cells. Variable selections for lipid annotation were based on S-Plot (C). Score plots of BAK-exposed and control cells are presented in both ESI+ (B1) and ESI- (B3). Metabolites with significant changes in cellular level between BAK-exposed and control cells are presented in ESI+ (C1) and ESI- (C3) S-plots (orange boxes delimited the variables of interest). Score plots of HO-exposed and control cells are presented in both ESI+ (B2) and ESI- (B4) ion mode. Metabolites with significant changes in cellular level between HO-exposed and control cells are presented in ESI+ (C2) and ESI- (C4) S-plots (orange boxes delimited the variables of interest).

Figure 4: Comparative cell lipid levels in HCE exposed to BAK or HO. (A) Change in discriminant lipid species in HCE cells exposed to BAK or HO. Results are expressed as fold changes compared to control (FDR-adjusted $p < 0.01$). Blue color corresponds to a decrease in the cell lipid level compared to control while red color indicates an increase. (B) Venn diagram displays common and specific modulated lipid species to BAK or HO HCE exposure. (C) Distribution of the total lipid classes between control, BAK and HO exposed HCE cells.

Figure 5: Alteration of sphingolipid metabolism. (A) Total ceramide and sphingomyelin level change following BAK or HO exposure (B) Metabolic pathways of sphingolipids. (C) Gene expression of enzyme involved in sphingolipid metabolism. Results are expressed as mean ± SD (ANOVA with Tukey's multiple comparisons test. n=5. *p < 0.05; **p < 0.01; ***p < 0.001).

Figure 6: Alteration of glycerolipid metabolism. (A) Change in total DG and TG levels following BAK or HO exposure. (B) Metabolic pathways of glycerolipids. (C) Gene expression of *DGAT1*, enzyme involved in TG biosynthesis. Results are expressed as mean ± SD (ANOVA with Tukey's multiple comparisons test. n=5. *p < 0.05; **p < 0.01; ***p < 0.001).

Figure 7: Alteration of glycerophospholipid metabolism. (A) Change in total PC and LPC levels following BAK or HO exposure. (B) Metabolic pathways of lipids containing choline head group. (C) Gene expression of *PLA1* which is implicated in LPC degradation to glycerylphoshorylcholine. (D) PLA2 activity change following BAK or HO exposure. Results are expressed as mean ± SD (ANOVA with Tukey's multiple comparisons test. n=5. *p < 0.05; **p < 0.01; ***p < 0.001).

Figure 8: Synopsis highlighting the main changes in lipid subclasses related to BAK and HO exposure. BAK and HO shared alterations are displayed in the white box at the center. Those specific to BAK and HO are respectively shown on the left and right side of the diagram.

737 **Figure 1**

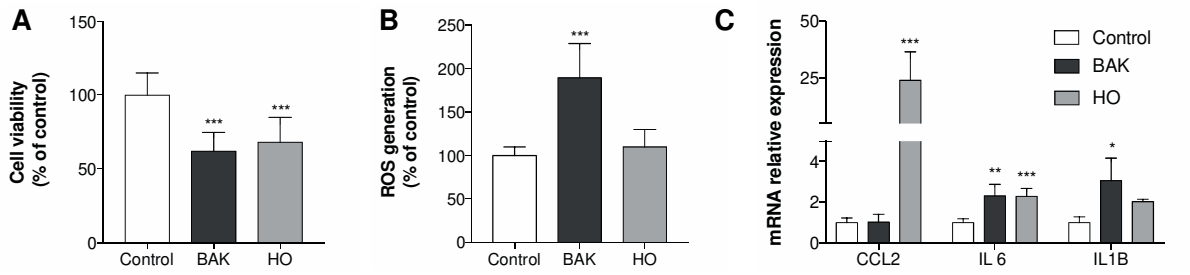

738
739

740 **Figure 2**

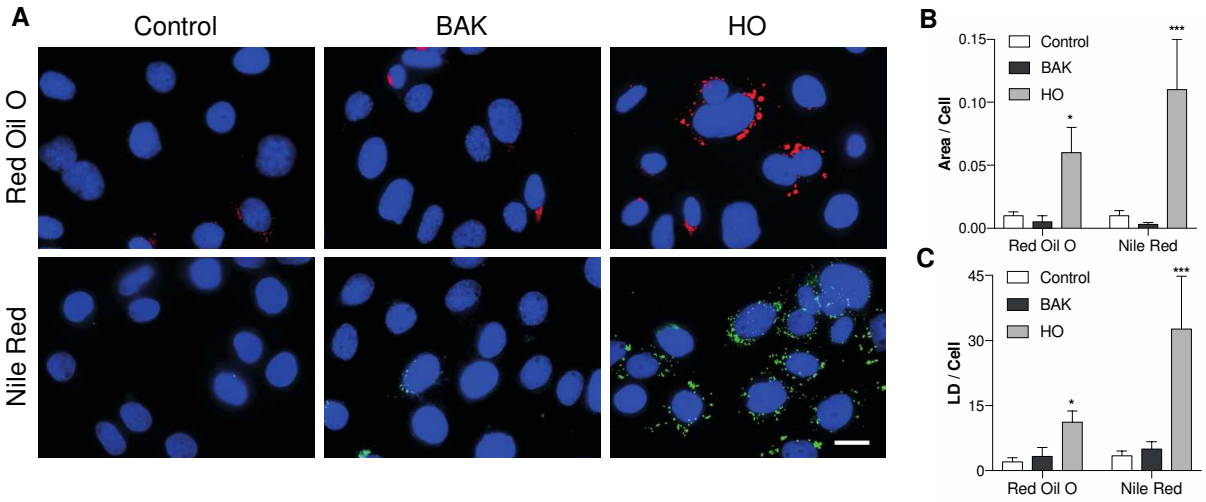

741
742

743 **Figure 3**

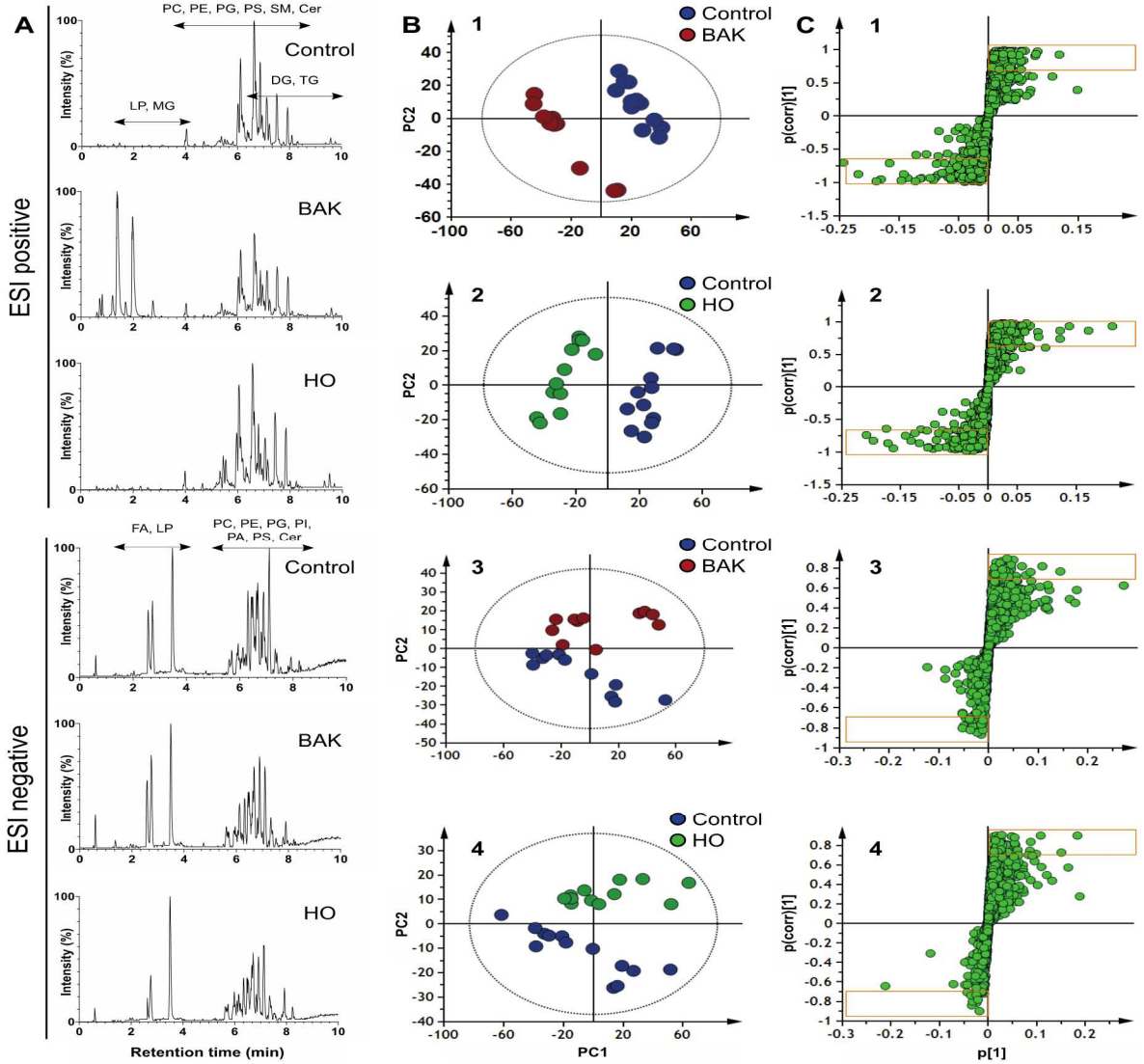

744
745

746 **Figure 4**

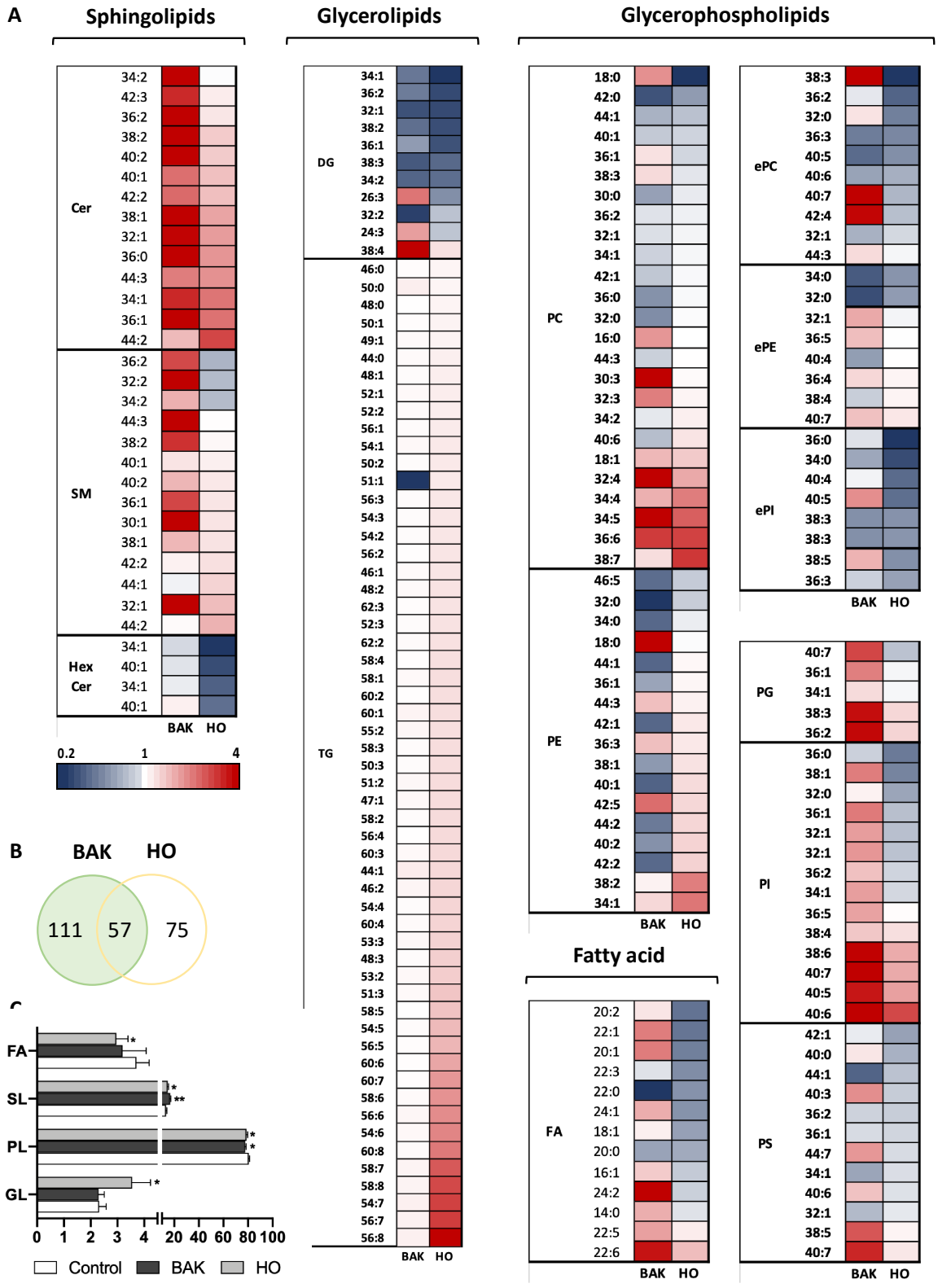

747

748 **Figure 5**

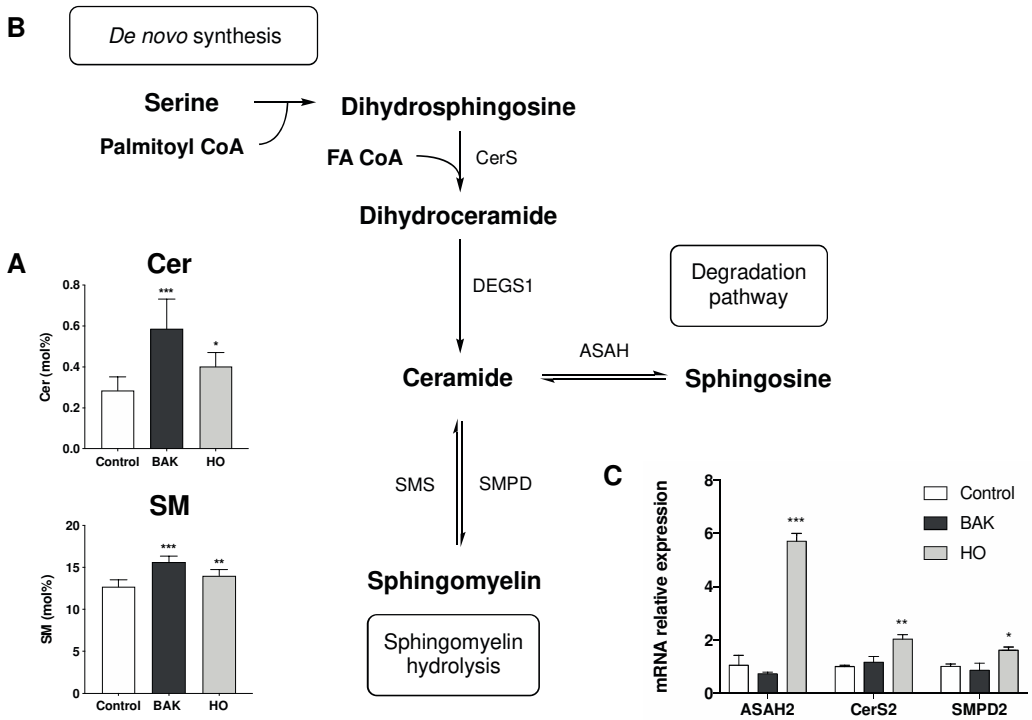

749

Figure 6

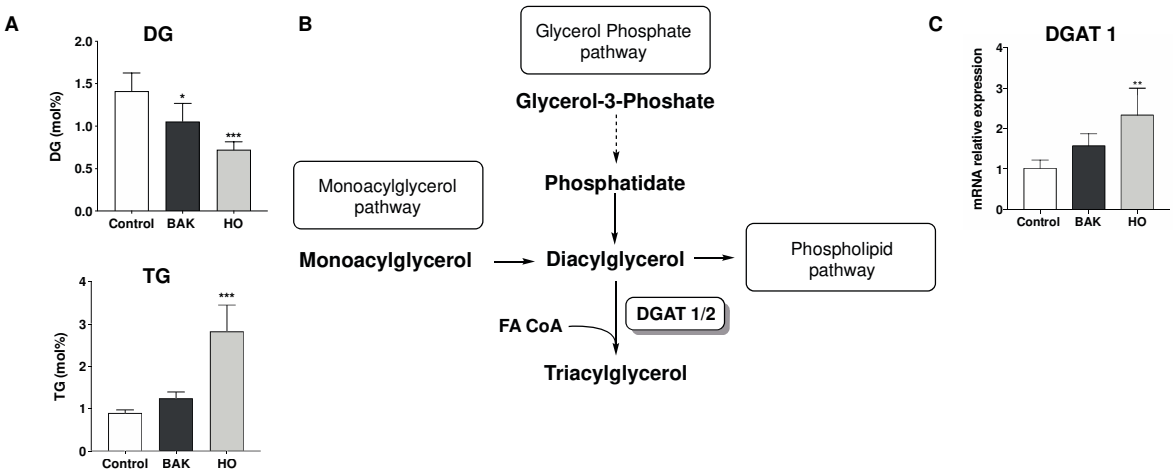
A
DG
DG (mol%)
2.0
1.5
1.0
0.5
0.0
*
***
Control
BAK
HO
TG
TG (mol%)
4
3
2
1
0
***
Control
BAK
HO
B
Glycerol Phosphate pathway
Glycerol-3-Phoshate
Monoacylglycerol pathway
Phosphatidate
Monoacylglycerol
Diacylglycerol
Phospholipid pathway
FA CoA
DGAT 1/2
Triacylglycerol
C
DGAT 1
mRNA relative expression
4
3
2
1
0
**
Control
BAK
HO

753 **Figure 7**

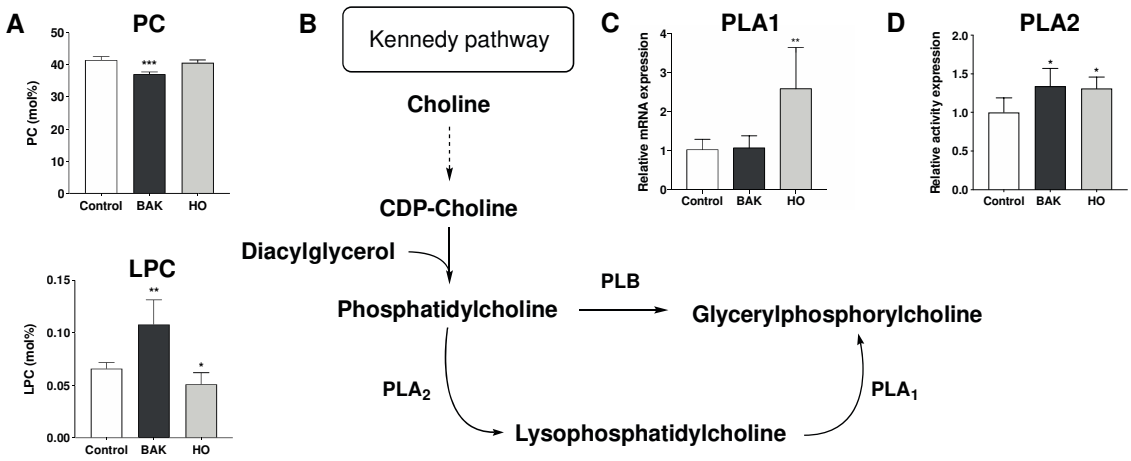

754

Figure 8

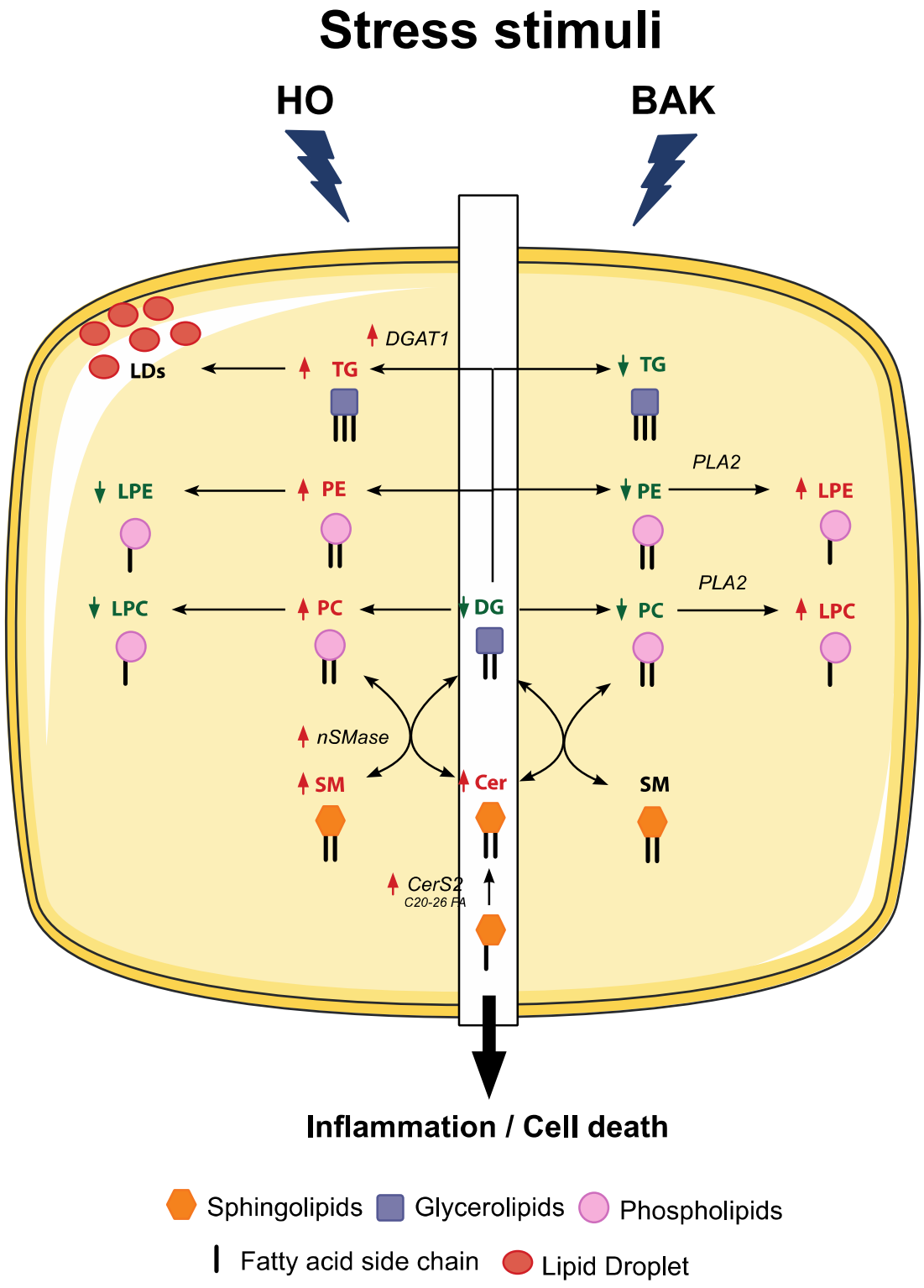
Stress stimuli
HO
BAK
LDs
DGAT1
TG
TG
PLA2
LPE
PE
PE
LPE
PLA2
LPC
PC
DG
PC
LPC
nSMase
SM
Cer
SM
CerS2
C20-26 FA
Inflammation / Cell death
Sphingolipids
Glycerolipids
Phospholipids
Fatty acid side chain
Lipid Droplet